

## ACOUSTIC PARAMAGNETIC RESONANCE IN FERROELECTRICS: $\text{Cr}^{3+}$ AND $\text{Nd}^{3+}$ IN POLY-DOMAIN $\text{LiNbO}_3$

U. Kh. KOPVILLEM and B. P. SMOLYAKOV

Kazan' Physico-technical Institute, USSR Academy of Sciences

Submitted July 31, 1968

Zh. Eksp. Teor. Fiz. 55, 2188–2194 (December, 1968)

An investigation has been carried out for the first time of the structure and dynamics of the internal fields of ferroelectric single crystals, using the acoustic electron paramagnetic resonance method. Resonance absorption of hypersound by the spin systems of  $\text{Cr}^{3+}$  and  $\text{Nd}^{3+}$  ions was found; this absorption is dependent on the magnetic field strength. The values of a number of elements of the spin-phonon interaction tensor are estimated for these ions. Comparison of these values with similar quantities for  $\text{Cr}^{3+}$  and  $\text{Nd}^{3+}$  in other, non-ferroelectric matrices shows that an amplification of the interaction between spin and lattice variables takes place in ferroelectric single crystals. This circumstance made it possible to discover acoustic magnetic resonance on the  $\text{Nd}^{3+}$  ion. Acoustic magnetic resonance on  $\text{Co}^{2+}$  in astrakhanite and  $\text{Cu}^{2+}$  in copper sulfate is also observed.

ACOUSTIC paramagnetic resonance (APR), predicted by Al'tshuler,<sup>[1]</sup> is widely used in the study of the fine details of the dynamics of internal crystalline fields in dielectric materials.<sup>[2]</sup> In contrast to the usual magnetic resonance, resonance transitions of APR are due to hypersound, which cannot interact directly with the spins, but which affects these degree of freedom through a complicated chain of internal couplings, including spin-orbit, exchange, contact and other electromagnetic interactions. This circumstance increases on the one hand the amount of information contained in the APR signal concerning the properties of materials, and on the other causes these signals to be weak and accordingly increases the experimental difficulties of their observation. In the present work, an attempt is made to use the APR method for a study of the dynamics of the internal fields in ferroelectrics. At the beginning of our investigations, virtually nothing was known about the generation and damping of sound of frequency  $\nu = 10^{10}$  Hz in ferroelectrics, as well as the possibility of transfer of hypersound from quartz to the ferroelectric. Experiments on the generation of hypersound at liquid helium temperatures in quartz,  $\text{LiTaO}_3$ ,  $\text{KH}_2\text{PO}_4$ , and  $\text{LiNbO}_3$  have shown that the latter two matrices are promising for the study of APR on impurities.<sup>[3]</sup> Further experiments led to the discovery of APR on  $\text{Cr}^{3+}$ <sup>[4]</sup> and  $\text{Nd}^{3+}$  ions in poly-domain single crystals of  $\text{LiNbO}_3$ . An analysis is given below of information obtained from the APR spectra of  $\text{Cr}^{3+}$  and  $\text{Nd}^{3+}$  ions.

The experiments were carried out at liquid helium temperatures with a previously-described hypersonic magnetic spectrometer.<sup>[3]</sup> Longitudinal hypersonic waves of frequency  $\nu = 10^{10}$  Hz were excited at the end of a X-cut quartz cylinder (length 15 mm, diameter 3 mm). The acoustic contact of the quartz with the lithium niobate was by means of a bond of ED-6 epoxy resin with the addition of a plasticizer. Three poly-domain samples were studied, in the form of cylinders with faces that were optically flat and parallel within  $10''$ . Sample I contained 0.05 at. %  $\text{Cr}^{3+}$  impurity. Its axis was perpendicular to the optical axis of the crystal

$c_3$ , while the G axis was directed perpendicular to the plane of reflection passing through the  $c_3$  axis. Sample II also contained 0.05 at. %  $\text{Cr}^{3+}$  impurity, but the z axis of the cylinder was parallel to  $c_3$ . Sample III contained 1 at. %  $\text{Nd}^{3+}$  impurity and was cut similar to sample I.

Resonance absorption of the hypersound was observed by measurement of the intensity of one of the reflected sound pulses passing through the  $\text{LiNbO}_3$  sample, as a function of a linearly changing magnetic field  $0 \leq H_0 \leq 10$  kG (see<sup>[4]</sup>). In the case of samples I and III, the field  $H_0$  made an angle  $0 \leq \theta \leq 90^\circ$  with the  $c_3$  axis, while for II the field  $H_0$  lay in the (xy) plane perpendicular to  $c_3$  and made an angle  $0 \leq \varphi \leq 360^\circ$  with the x axis. The crystallographic structure of  $\text{LiNbO}_3$  is a complicated variant of the well studied structure of  $\text{Al}_2\text{O}_3$ . In the paraelectric phase ( $T > T_C = 1210^\circ\text{C}$ ), both lattices have the symmetry  $C_{3d}$ <sup>[5]</sup> and the structure of  $\text{LiNbO}_3$  is obtained from the structure of  $\text{Al}_2\text{O}_3$  by the replacement of one of the atoms of aluminum by Li and the other by Nb. In the phase transition, the mean value of the displacement of the Li and Nb atoms from the center of inversion position in the lattice becomes different from zero. This displacement is the ordering parameter of Landau and Lifshitz<sup>[6]</sup> and transforms the group of invariant transformations  $C_{3d}$  to the group  $C_{3v}$  which is a subgroup of  $C_{3d}$ . The  $\text{LiNbO}_3$  crystal can be described by means of a rhombohedral unit cell of volume  $106.074 \text{ \AA}^3$  which contains two  $\text{LiNbO}_3$  molecules in non-equivalent positions. The density of the crystal  $\rho = 4.640 \text{ g-cm}^{-3}$  at  $4^\circ\text{C}$  and the number of Li atoms in  $1 \text{ cm}^3$  is equal to  $N = 1.89 \times 10^{22} \text{ cm}^{-3}$ . According to the  $C_{3v}$  symmetry, there exists in the  $\text{LiNbO}_3$  crystal a preferred direction  $\mathbf{z} \parallel c_3$  and a direction  $\mathbf{G}$  which is perpendicular to one of the three reflection planes passing through  $c_3$ . The local symmetry in the lattice sites of Li and Nb is described by the group  $C_3$  and in the lattice sites of the oxygen by the group  $C_1$ . There are two types of sites in the unit cell, in which the Li and Nb can be located. We shall denote them by the indices a and b. The oxygen environment of Li in the position a is obtained from position b by a reflection in the plane

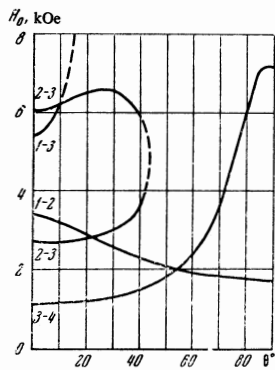


FIG. 1. Dependence of the resonance magnetic field on the angle  $\theta$  between  $c_3$  and the magnetic field for a frequency of 9.3 GHz in the case of  $Cr^{3+}$  in  $LiNbO_3$ . The states 1, 2, 3 and 4 in a strong field correspond to the spin functions  $| -1/2 \rangle$ ,  $| +1/2 \rangle$ ,  $| -3/2 \rangle$  and  $| +3/2 \rangle$



FIG. 3. EPR spectrum of the  $Cr^{3+}$  ion in  $LiNbO_3$  at room temperature for  $\theta = 20^\circ$ . The static magnetic field increases from left to right (the distance from the arrow to the maximum of the fundamental line amounts to  $\approx 1650$  G). The arrow indicates the forbidden transition  $| +3/2 \rangle \leftrightarrow | -3/2 \rangle$ . The fundamental line corresponds to the transition  $| +1/2 \rangle \leftrightarrow | -1/2 \rangle$ . To it on the right side is added the transition  $| +1/2 \rangle \leftrightarrow | -3/2 \rangle$ . The line  $| +1/2 \rangle \leftrightarrow | -3/2 \rangle$  is seen again further along at high fields.

perpendicular to the  $c_3$  axis, with subsequent rotation of the upper and lower oxygen triplets in different sides around the  $c_3$  axis with the simultaneous contraction of the distance between the atoms of one triplet and an increase in the distances in the other triplet. Thus the spin-phonon interaction tensor in the fixed system of coordinates (x, y, z) in the positions a and b is shown to be different in magnitude. In corundum, the corresponding elements in the positions a and b have the same absolute magnitudes and only some of them have opposite signs.<sup>[7]</sup>

APR ON  $Cr^{3+}$  IN  $LiNbO_3$

EPR studies have shown that the impurity  $Cr^{3+}$  ions occupy the sites of Li or Nb, while all the  $Cr^{3+}$  impurity ions are magnetically equivalent.<sup>[8,9]</sup> The internal crystalline field is described by the axial spin Hamiltonian  $\mathcal{H}_S = D[S_z^2 - (1/3)S(S+1)]$ , where  $S = 3/2$  is the spin of  $Cr^{3+}$  and  $D = 0.45$  cm<sup>-1</sup>. Let the energy levels  $E_\alpha$  ( $\alpha = 1, \dots, 4$ ) of the  $Cr^{3+}$  in a strong field  $H_0$  refer respectively to the states  $| 3/2 \rangle$ ,  $| 1/2 \rangle$ ,  $| -1/2 \rangle$  and  $| -3/2 \rangle$  (see<sup>[10]</sup>). Figure 1 shows the dependence of the resonance field  $H_0$  for the transitions 3-4, 2-3, 1-2, 1-3 and 2-3 as functions of the angle  $\theta$  in the case of variable magnetic-field frequency  $\nu = 9.3$  GHz, as obtained

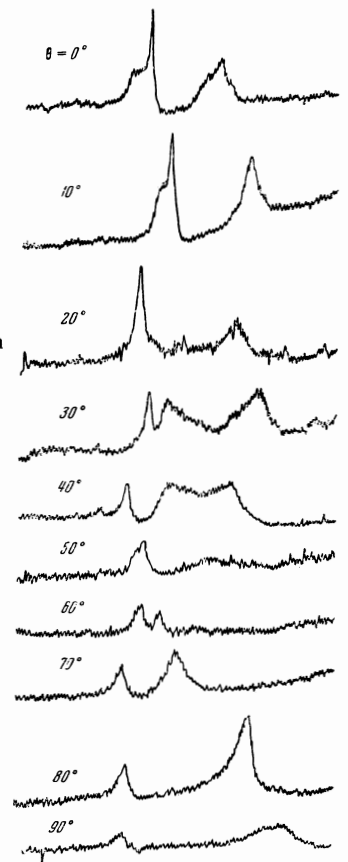


FIG. 2. APR spectra on  $Cr^{3+}$  in  $LiNbO_3$  on sample I at 4.2°K in field on 0-10<sup>4</sup> G as a function of the angle  $\theta$  between the  $c_3$  axis and the magnetic field. Longitudinal sound waves are propagated perpendicular to the direction of the field.

by L. P. Litovkina and M. L. Meil'man. Figure 2 shows the APR spectra of sample I for  $0 \leq \theta \leq \pi/2$  and the corresponding data for the hypersound damping coefficient  $\alpha$  are shown in the table. This damping is due to the interaction with the  $Cr^{3+}$  ions. By comparison of Figs. 1 and 2, and also with the EPR data, it was established that all the transitions shown in Fig. 1 were observed by the APR method.

Figure 3 shows the first derivatives of the ordinary EPR signal at room temperature for  $\theta = 20^\circ$  on  $Cr^{3+}$  ions. Comparison of Fig. 2 and Fig. 3 shows that the line intensities in APR and EPR spectra are completely different. There is only one intense EPR line in Fig. 3, corresponding to the transition  $| 1/2 \rangle \leftrightarrow | -1/2 \rangle$ , which agrees with the results of the work of Evlanova et al.<sup>[9]</sup>

The form of the spin Hamiltonian  $\mathcal{H}_S$  for the EPR spectrum of  $Cr^{3+}$  in  $LiNbO_3$  is close to  $\mathcal{H}_S$  for  $Cr^{3+}$  in  $Al_2O_3$ . Therefore, it is natural to attempt to interpret the APR data on the basis of the effective spin-phonon interaction operator  $\mathcal{H}_{SL}$ , which characterizes the

Absorption coefficients  $\alpha$  and line widths  $\Delta H$  for different APR transitions of the  $Cr^{3+}$  ion in  $LiNbO_3$  at 4.2°K

$\theta^\circ$	Transition	$\alpha, \text{cm}^{-1}$	$\Delta H, \text{G}$	$\theta^\circ$	Transition	$\alpha, \text{cm}^{-1}$	$\Delta H, \text{G}$
0	$1/2 \rightarrow -3/2$	0,09	300	60	$1/2 \rightarrow -3/2$	0,14	800
	$1/2 \rightarrow -1/2$	0,27	135		$1/2 \rightarrow -3/2$	0,15	870
	$-1/2 \rightarrow -3/2$	0,08	500	90	$3/2 \rightarrow -3/2$	0,1	290
	$1/2 \rightarrow -3/2$	0,1	340		$1/2 \rightarrow -1/2$	0,09	235
30	$3/2 \rightarrow -3/2$	0,05	190	90	$1/2 \rightarrow -1/2$	0,03	290
	$1/2 \rightarrow -1/2$	0,16	235		$3/2 \rightarrow -3/2$	0,06	1330

Van Vleck mechanism and which is dominant for  $\text{Cr}^{3+}$  in  $\text{Al}_2\text{O}_3$ .<sup>[7,11]</sup> The operator  $\mathcal{H}_{\text{SL}}$  has the form

$$\mathcal{H}_{\text{SL}} = d_{xx}S_x^2 + d_{yy}S_y^2 + d_{zz}S_z^2 + d_{yz}(S_zS_y + S_yS_z) + d_{xz}(S_zS_x + S_xS_z) + d_{xy}(S_yS_x + S_xS_y),$$

$$d_{\alpha\beta} = \sum_{\gamma, \delta} G_{\alpha\beta\gamma\delta} \epsilon_{\gamma\delta}, \quad (1)$$

where  $G_{\alpha\beta\gamma\delta}$  is the spin-phonon interaction tensor<sup>[11]</sup> and  $\epsilon_{\gamma\delta}$  is the deformation tensor.

For  $C_3$  symmetry, the tensor  $G$  has the form

$$G = \begin{pmatrix} G_{11} & G_{12} & -G_{33} & G_{14} & G_{15} & -2G_{16} \\ G_{12} & G_{11} & -G_{33} & -G_{14} & -G_{15} & -2G_{16} \\ -(G_{11} + G_{12}) & -(G_{11} + G_{12}) & 2G_{33} & 0 & 0 & 0 \\ G_{41} & -G_{41} & 0 & G_{44} & G_{45} & 2G_{46} \\ -G_{16} & G_{46} & 0 & -G_{45} & G_{44} & 2G_{41} \\ -G_{16} & G_{16} & 0 & -G_{15} & G_{14} & (G_{11} - G_{12}) \end{pmatrix} \quad (2)$$

where the contracted Voigt notation is used.

Let  $G^{(a)}$  and  $G^{(b)}$  be the tensors  $G$  for positions  $a$  and  $b$ , respectively, of the  $\text{Cr}^{3+}$  ions in  $\text{LiNbO}_3$ . In the case of  $\text{Cr}^{3+}$  in  $\text{Al}_2\text{O}_3$ , only the elements  $G_{46}$ ,  $G_{16}$ ,  $G_{15}$ ,  $G_{45}$  reverse sign on going from position  $a$  to position  $b$ , while  $G_{46} = G_{16} = 0$ . For longitudinal sound waves propagating along the  $x$  axis, the absorption coefficient  $\alpha_{\text{cd}}$  for the transition  $|c\rangle \leftrightarrow |d\rangle$  is computed according to the formula

$$\alpha_{\text{cd}} = \frac{\pi \Delta n_{\text{cd}} \nu_{\text{cd}} g_{\text{cd}}(\nu)}{2 \rho v_{\text{xx}}^3 \epsilon_{\text{xx}}^2 \hbar} \{ |\langle c | \mathcal{H}_{\text{SL}}^{I(a)} | d \rangle|^2 + |\langle c | \mathcal{H}_{\text{SL}}^{I(b)} | d \rangle|^2 \}$$

$$\mathcal{H}_{\text{SL}}^{I(\xi)} = \epsilon_{\text{xx}} \{ G_{11}^{(\xi)} S_x^2 + G_{12}^{(\xi)} S_y^2 - (G_{11}^{(\xi)} + G_{12}^{(\xi)}) S_z^2 + G_{41}^{(\xi)} (S_z S_y + S_y S_z) + (-G_{15}^{(\xi)}) (S_y S_x + S_x S_y) + (-G_{46}^{(\xi)}) (S_x S_z + S_z S_x) \}, \quad \xi = a, b, \quad (3)$$

where  $\Delta n_{\text{cd}}$  is the population difference in levels  $E_d > E_c$  per unit volume,  $\nu_{\text{cd}}$  is the resonance frequency,  $g_{\text{cd}}(\nu)$  is a form factor,  $\rho$  is the density of the crystal,  $v_{\text{xx}}$  is the speed of longitudinal sound waves along the  $x$  axis, and  $\langle c | \mathcal{H}_{\text{SL}}^{I(\xi)} | d \rangle$  is the matrix element.

In the case of longitudinal waves propagating along the  $z$  axis, it is necessary to carry out the computations according to (3) with the replacement of  $v_{\text{xx}}$  by  $v_{\text{zz}}$ ,  $\epsilon_{\text{xx}}$  by  $\epsilon_{\text{zz}}$ , and  $\mathcal{H}_{\text{SL}}^{I(\xi)}$  by

$$\mathcal{H}_{\text{SL}}^{II(\xi)} = \epsilon_{\text{zz}} G_{33}^{(\xi)} (-S_x^2 - S_y^2 + 2S_z^2)/2. \quad (4)$$

Investigations of EPR on  $\text{Cr}^{3+}$  ions in  $\text{LiNbO}_3$  have shown<sup>[8,9]</sup> that the intensity of these lines is roughly described by the Hamiltonian  $\mathcal{H}_{\text{S}}$ , and a "rhombic" term of the type  $E(S_x^2 - S_y^2)$  can enter into it. However, the great line width and the absence in the EPR spectrum of intense lines other than  $|1/2\rangle \leftrightarrow |-1/2\rangle$  made it impossible to find the terms  $E(S_x^2 - S_y^2)$ . In the case of APR, the line width was greater than for EPR. Therefore, in an estimate of the elements  $G_{\alpha\beta}^{(\xi)}$ , we neglected the difference  $|G_{\alpha\beta}^{(a)}| \neq |G_{\alpha\beta}^{(b)}|$  and in Eqs. (3) and (4), we estimated the average values of these elements. In the calculations, we used wave functions from<sup>[10]</sup> with account of the difference in the  $D$  constants for  $\text{Cr}^{3+}$  in  $\text{LiNbO}_3$  and  $\text{Al}_2\text{O}_3$ . The following choice of values of  $G_{\alpha\beta}$  (in units of  $10^{-16}$  erg/unit deformation) gave the best agreement with the experimental data:  $G_{11} = 77 \pm 1$ ,  $G_{12} = 75 \pm 1$ ,

$G_{14} = -81 \pm 1$ ,  $G_{16} = 5.9 \pm 0.1$ ,  $G_{46} = 1.4 \pm 0.1$ , and  $|G_{33}| = 1.2 \pm 0.1$ . The width of the APR lines cannot be explained by the contribution from magnetic dipole-dipole interactions ( $\text{Cr}^{3+} - \text{Cr}^{3+}$ ,  $\text{Cr}^{3+} - \text{Li}^7$ ,  $\text{Cr}^{3+} - \text{Li}^6$ ,  $\text{Cr}^{3+} - \text{Nb}^{93}$ ). For the observed transitions, these mechanisms give a frequency width  $\Delta\nu \sim (11 \times 10^6 - 29 \times 10^6) \text{ sec}^{-1}$  at half intensity, which is smaller by an order of magnitude than the experimental values. Evidently the width of the APR lines is due to the scatter in the constants of the spin Hamiltonian  $\mathcal{H}_{\text{S}}$ , to the block and mosaic structures of the samples, but not to the poly-domain structure of these crystals.

#### APR ON $\text{Nd}^{3+}$ IN $\text{LiNbO}_3$

EPR spectrum of  $\text{Nd}^{3+}$  in  $\text{LiNbO}_3$  was observed by Evlanova et al. in<sup>[9]</sup>. The single crystal contains  $\text{Nd}^{3+}$  in two non-equivalent positions. For  $\mathbf{H}_0 \perp c_3$ , the  $g$  factors  $g = 2.95 \pm 0.05$  of these non-equivalent ions are identical, while for  $\mathbf{H}_0 \parallel c_3$ ,  $g'_{\parallel} = 1.43 \pm 0.02$  and  $g''_{\parallel} = 1.33 \pm 0.02$  are obtained. So far as APR spectrum of the  $\text{Nd}^{3+}$  ion is concerned, it has not been observed to date in any one of the crystals studied, although APR experiments have been carried out on  $\text{Nd}^{3+}$  in  $\text{CaF}_2$ ,<sup>[11]</sup> and also by us. The effective spin of the  $\text{Nd}^{3+}$  ion is  $S = 1/2$  and its operator of spin-phonon interaction  $\mathcal{H}_{\text{SL}}$  depend on the intensity of the static magnetic field  $H_0$  (it is obtained from (1) by replacing of one of the  $S_{\alpha}$  by the component  $H_{0\alpha}$  of the field  $H_0$ , and  $G_{\alpha\beta\gamma\delta}$  by  $F_{\alpha\beta\gamma\delta}$ ). The absence of APR signal from  $\text{Nd}^{3+}$  in  $\text{CaF}_2$  and in scheelite ( $\text{CaWO}_4$ ) can be explained by the small value of the quantity  $F_{\alpha\beta}$ . In our  $\text{LiNbO}_3$  crystal, the APR lines of the  $\text{Nd}^{3+}$  ion can be observed only for  $\theta = 90^\circ$ , and half a half-width of  $\Delta H \sim 80$  G. Applying Eq. (3), we estimated the value of the elements  $F_{\alpha\beta} \sim 3 \times 10^{-19}$  erg/deformation unit-Gauss.

Calculation of the contributions of the dipole-dipole interactions ( $\text{Nd}^{3+} - \text{Nd}^{3+}$ ,  $\text{Nd}^{3+} - \text{Li}^7$ ,  $\text{Nd}^{3+} - \text{Li}^6$ ,  $\text{Nd}^{3+} - \text{Nb}^{93}$ ) give a value of the frequency width of the APR line  $\Delta\nu \sim 0.4 \times 10^8 \text{ sec}^{-1}$ , which is smaller by a factor of ten than the observed value. The additional broadening can be explained by the unresolved hyperfine structure, by the mixing of the APR lines from two non-equivalent  $\text{Nd}^{3+}$  ions and by the scatter in the directions of the axes  $c_3$ .

#### DISCUSSION OF THE RESULTS

The data for the  $\text{Cr}^{3+}$  ion show that the mechanism of spin-phonon interaction, which is described by the elements of the tensor  $G_{\alpha\beta}$ , is effective both in  $\text{LiNbO}_3$  and in  $\text{Al}_2\text{O}_3$ . As is known, the Van Vleck mechanism<sup>[12]</sup> consists of the production of oscillations of the crystalline field at the  $\text{Cr}^{3+}$  ions by the sound field, while this internal field is created by the neighboring regions about the  $\text{Cr}^{3+}$  ion. On the other hand, experiments with ordinary EPR in ferroelectrics show that the constants of the spin Hamiltonian are insignificantly changed in the transition through the phase point, in view of the fact that the field from the spontaneous electric polarization makes little contribution to the crystalline field on paramagnetic impurities. It then follows that in an ordered electric state, the elements  $G_{\alpha\beta}$  will have approximately the same value as in a disordered state.

Comparison of the elements  $G_{\alpha\beta}$  for  $\text{Cr}^{3+}$  in  $\text{Al}_2\text{O}_3$  and  $\text{LiNbO}_3$  shows that in  $\text{LiNbO}_3$ , the mean  $G_{\alpha\beta}$  are somewhat larger than in  $\text{Al}_2\text{O}_3$ . This can be explained by the fact that in  $\text{LiNbO}_3$  the crystalline field is less symmetric and more dynamic than in  $\text{Al}_2\text{O}_3$ , and by the fact that the D constant in  $\text{LiNbO}_3$  is larger than in corundum. As was noted in<sup>[4]</sup>, the dependence of the damping coefficient  $\alpha$  on the angle  $\theta$  for the transition  $|1/2\rangle \leftrightarrow |-1/2\rangle$ , and also its value at  $\theta = 0$ , do not agree with the predictions of the Van Vleck mechanism and with the form of  $\mathcal{H}_S$ . In the first place, this can be due to the specific property of spin-phonon interaction in the ferroelectric phase, when the magnetic particle moves close to the domain boundaries under the influence of the elastic oscillations, interacting with the induction electromagnetic field. Second, in the case of the presence of rhombic terms of the type  $E(S_x^2 - S_y^2)$  in the spin Hamiltonian, the orientation  $\theta = 0$ , for which the states of  $\text{Cr}^{3+}$  are eigenfunctions of the operator  $S_z$ , generally "does not exist."

Such a conclusion is confirmed by the following facts: a) in the ordinary EPR spectrum of the  $\text{Cr}^{3+}$  ion in  $\text{LiNbO}_3$  at  $\theta = 0^\circ$ , a "forbidden" line  $|3/2\rangle \leftrightarrow |-3/2\rangle$  is observed; in the APR spectrum of the  $\text{Cr}^{3+}$  line in lithium niobate, for acoustic deformations  $\epsilon_{zz} \cos \omega t$  and for rotation of the field  $H_0$  in the xy plane, a periodic change is observed in the width of the APR line (with a period of  $120^\circ$ ) for sample II. For such a situation, analogous to the "forbidden line"  $|3/2\rangle \leftrightarrow |-3/2\rangle$  for EPR, a line that is "forbidden" for APR,  $|1/2\rangle \leftrightarrow |-1/2\rangle$ , can be seen. The selection rules for this line will be satisfied by the addition of  $E(S_x^2 - S_y^2)$ ; however, in the first approximation relative to the unexcited spin Hamiltonian, the contribution from the mechanisms of inhomogeneous broadening will be absent from it. This can lead to a growth in its intensity relative to other lines and other sites  $\theta \neq 0^\circ$ , since in these cases, some of the  $\text{Cr}^{3+}$  ions cannot generally take part in the resonance because of the large scatter in the constant D.<sup>[13]</sup> Since the APR and EPR line widths are not governed by the domain structure, upon improvement in the techniques of crystal growth of these single crystals, they may turn out to be useful materials for acoustic masers. We note that the NMR line widths for  $\text{Li}^7$  and  $\text{Nb}^{93}$  in  $\text{LiNbO}_3$  also possess properties that are not understood: for  $\text{Li}^7$  the line width is explained by the magnetic  $\text{Li}^7 - \text{Nb}^{93}$  dipole-dipole interaction, and in the case of NMR on  $\text{Nb}^{93}$ , an unexplained broadening and disappearance of the line  $|1/2\rangle \leftrightarrow |-1/2\rangle$  are observed upon increase of the angle  $\theta \neq 0$ . Therefore, the reasons for the line broadening of the magnetic and acoustic resonances in lithium niobate require a more detailed investigation.

The discovery of APR in  $\text{LiNbO}_3$  on  $\text{Nd}^{3+}$  shows that the ferroelectric matrix for this ion is more satisfactory than the paramagnetic matrix. The value of  $F_{\alpha\beta}$  for  $\text{Nd}^{3+}$  in scheelite was estimated by Zaitov and

Shekun<sup>[14]</sup> by the pressure method and was shown to be equal to  $10^{-20}$  erg/deformation-unit-Gauss. It then follows that in the  $\text{CaWO}_4$  matrix, the APR intensity will not be sufficient for observation with the APR apparatus used. Therefore the study of APR on rare-earth ions in ferroelectric matrices is very promising.

We give below some preliminary results of the observation of APR at a frequency of  $10^{10}$  sec<sup>-1</sup> at  $4.2^\circ\text{K}$  in hydrous paramagnetic monocrystals. The resonance is observed in  $\text{Co}^{2+}$  ions in astrakhanite  $\text{Na}_2\text{Co}(\text{SO}_4)_2 \cdot 4\text{H}_2\text{O}$ . For the elements of the tensor  $F_{\alpha\beta}$ , we obtained the estimate  $0.42 \times 10^{-19}$  erg/deformation-unit-Gauss, and for sound modulation of the hyperfine structure constant,  $G_{\text{HSC}} \sim 1.2 \times 10^{-16}$  erg/deformation unit. The resonance absorption of the hypersound was also observed in  $\text{Cu}^{2+}$  ions in copper sulfate ( $\text{CuSO}_4 \cdot 5\text{H}_2\text{O}$ ). The elements  $F_{\alpha\beta} \sim 3 \times 10^{-19}$  erg/deformation-unit-Gauss.

<sup>1</sup>S. A. Al'tshuler, Dokl. Akad. Nauk SSSR 85, 1235 (1952).

<sup>2</sup>E. B. Tucker, Proc. IEEE 53, 1547 (1965).

<sup>3</sup>B. P. Smolyakov, Tezisy dokladov yubileinoi konferentsii KFTI AN SSSR (Papers of the Jubilee Conference, Kazan' Physico-technical Institute, Academy of Sciences, USSR) Kazan', 1966, p. 70. Materials of the VI All-Union Acoustics Conference, Moscow, 1968, Session EIII, 3.

<sup>4</sup>B. P. Smolyakov, M. L. Meil'man, V. P. Klyuev, I. A. Shpil'ko and U. Kh. Kopvillem, ZhETF Pis. Red. 7, 26 (1968) [JETP Lett. 7, 17 (1968)].

<sup>5</sup>A. S. Barker and R. Loudon, Phys. Rev. 158, 433 (1967).

<sup>6</sup>L. D. Landau and E. M. Lifshitz, Statisticheskaya fizika (Statistical Physics), Gostekhizdat, 1951 [Addison-Wesley, 1958].

<sup>7</sup>R. B. Hemphill, P. L. Donoho, E. D. McDonald, Phys. Rev. 146, 329 (1966), P. L. Donoho, Phys. Rev. 133, A1080 (1964).

<sup>8</sup>G. Burns, D. F. O'Kane and R. S. Title, Phys. Lett. 23, 56 (1966).

<sup>9</sup>N. F. Evlanova, L. S. Korinenko, L. N. Rashkovich and A. O. Rybaltovskii, Zh. Eksp. Teor. Fiz. 53, 1920 (1967) [Sov. Phys.-JETP 26, 1090 (1968)].

<sup>10</sup>J. Weber, Rev. Mod. Phys. 31, 681 (1959).

<sup>11</sup>W. I. Dobrov, Phys. Rev. 134, A734 (1964); 146, 268 (1966).

<sup>12</sup>J. H. Van Vleck, Phys. Rev. 57, 426 (1940).

<sup>13</sup>A. R. Kessel' and U. Kh. Kopvillem, Fiz. Tverd. Tela 5, 667 (1963) [Sov. Phys.-Solid State 5, 485 (1963)].

<sup>14</sup>M. M. Zaitov and L. Ya. Shekun, ZhETF Pis. Red. 4, 338 (1966) [JETP Lett. 4, 228 (1966)].